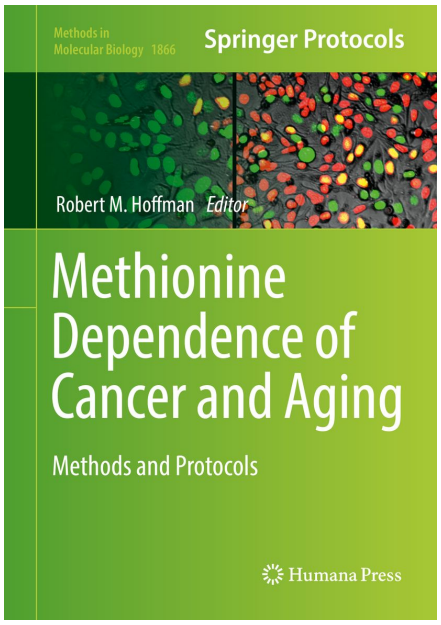

Humana Press

1st edition

Due 2019-02-04
1st ed. 2019, XII, 329 p. 80 illus., 34 illus. in color.

Printed book
Hardcover

Printed book
Hardcover
ISBN 978-1-4939-8795-5
$ 219,99

In production

Discount group
Professional Books (2)

Product category
Contributed volume

Series
Methods in Molecular Biology

Biomedicine : Cancer Research

Hoffman, Robert M. (Ed.), AntiCancer, Inc., San Diego, CA, USA

Methionine Dependence of Cancer and Aging

Methods and Protocols

- Includes cutting-edge methods and protocols
- Provides step-by-step detail essential for reproducible results
- Contains key notes and implementation advice from the experts

This book explores the methionine dependence of cancer and its effects on aging, a great story of science that is not widely known. The chapters in this book describe the discovery of methionine dependence of cancer; the molecular basis for the increased methionine demand of cancer cells and tumors; the clinical application of methionine dependence of cancer in PET imaging with [11C]methionine; the development of methioninases as cancer drugs; the anti-aging and anti-diabetes effects of methionine restriction; and the future of targeting methionine in the body for the elimination of cancer and for the extension of a healthy life-span. Written in the highly successful Methods in Molecular Biology series format, chapters include introductions to their respective topics, lists of the necessary materials and reagents, step-by-step, readily reproducible laboratory protocols, and tips on troubleshooting and avoiding known pitfalls. Cutting-edge and thorough, Methionine Dependence of Cancer and Aging: Methods and Protocols is an important resource for researchers and scientists wishing to pursue this exciting and vital area of study."

Order online at springer.com/booksellers
Springer Nature Customer Service Center LLC
233 Spring Street
New York, NY 10013
USA
T: +1-800-SPRINGER NATURE
(777-4643) or 212-460-1500
customerservice@springernature.com

ISBN 978-1-4939-8795-5 / BIC: MJCL / SPRINGER NATURE: SCB11001

METHIONINE DEPENDENCE OF CANCER AND AGING: METHODS AND PROTOCOLS, R.M. Hoffman, Editor
Chapter 18

Methionine gamma lyase from *Clostridium sporogenes* increases the anticancer effect of doxorubicin in A549 cancer cells in vitro and human cancer xenografts

Pokrovsky V.S.[1,2], Anisimova N.Yu.[1], Davydov D.Zh.[1], Bazhenov S.V.[3,4], Bulushova N.V.[3], Zavilgelsky G.B.[3], Kotova V.Y.[3], I.V. Manukhov[3,4]

[1] *Laboratory of combined treatment, N.N. Blokhin Cancer Research Center, Moscow, Russia*

[2] *Department of Biochemistry, People's Friendship University (RUDN University), Moscow, Russia*

[3] *State Research Institute of Genetics and Selection of Industrial Microorganisms, Moscow, Russia*

[4] *Laboratory of Molecular Genetics, Moscow Institute of Physics and Technology, Dolgoprudny, Moscow Region, Russia*

Abstract

The anti-cancer efficacy of methionine γ-lyase (MGL) from *Clostridium sporogenes* (*C. sporogenes*) is described. MGL was active against cancer cells in vitro and in vivo. Doxorubicin (DOX) and MGL were more effective on A549 human lung cancer growth inhibition than either agent alone in vitro and in vivo. The growth inhibitory effect of DOX + MGL on A549 xenograft *in vivo* was reflective of the results obtained *in vitro*.

Introduction

Methionine γ-lyase (MGL) [EC 4.4.1.11] is a pyridoxal 5'-phosphate-dependent enzyme, which catalyzes γ-elimination of L-methionine with the production of methyl mercaptan, α-ketobutyric acid, and ammonia. MGL is widely distributed in bacteria, and has been isolated from *Pseudomonas putida*, from the eukaryotic protozoa *Trichomonas vaginalis* and *Entamoeba histolytica*, from fungi *Aspergillus flavipes* and several other microorganisms [1]. The enzyme is promising as antitumor agent since methionine is required in excess for the growth of malignant cells [2]. MGLs from diverse microorganisms exhibited significant reduction of methionine *in vivo* have shown efficacy against a wide spectrum of transplantable animal and human solid tumors [3] (Note 1).

The first MGL was isolated from *Clostridium sporogenes* (*C. sporogenes*), was by Kreis and Hession [4]. This MGL inhibited growth of P815 cells in vitro cultures and the Walker carcinosarcoma 256 of the rat in vivo. Compared with a methionine-free diet, this enzyme had greater growth-inhibiting activity and negligible toxicity when evaluated by weight loss of the host. Semipurified MGL reduced plasma methionine to below 8% of the control [4].

MGL from *P. putida* is the most extensively studied MGL [3]. *P. putida* MGL inhibited growth of the murine Lewis lung carcinoma in mice [5], human colon cancer xenografts [6] and glioblastoma [7] in many studies and in patient-derived orthotopic xenografts (PDOX) recently [8-10]. Antitumor activity of the enzyme from *A. flavipes* with respect to several human tumors was observed *in vivo* [11]. MGL enhanced the efficacy of doxorubicin (DOX) [12], 5-fluorouracil (5-FU) [5], cisplatinum (CDDP) [6], and nitrosoureas [7, 13, 14]. MGL from *P. putida* in combination with cisplatin, 5-fluorouracil (5-FU), and 1,3-bis(2-chloroethyl)-1-nitrosourea (BCNU) in mouse models of colon cancer, lung cancer, and brain cancer.

Recently *MGL* gene from *C. sporogenes* was cloned, and the recombinant enzyme was purified and characterized [15]. Previous studies have evaluated the cytotoxic effect of MGL, in PC-3 prostate cancer and K562 human chronic erythroblastic leukemia cell cultures, were sensitive to MGL from *C. sporogenes*; with IC_{50} values 0.1–0.4 and 0.4–1.3 U/ml, respectively [15] (**Note 1**).

MATERIALS

- *Escherichia coli* strain BL21 (DE3) F- *ompT hsdS* B *gal dcm* (DE3) (Novagen)
- *C. sporogenes* MGL gene
- *E. coli* strain K12 AB2463
- L-broth
- Agar medium
- Kanamycin
- KFK-2MP photocolorimeter
- *E. coli* MDG1216 strain
- Plasmid pET-mgl-Sporog
- Glycerol
- Tryptone (11.3 g/l)
- Yeast extract (5.6 g/l)
- ANCUM-2M fermenter (Institute of Biological Instrumentation of RAS, Pushchino)
- Potassium-phosphate buffer with 0.001 M Na_4EDTA
- DTT
- Pyridoxal phosphate
- APV-1000 disintegrator
- PMSF solution
- Q-Sepharose column
- A VivaFlow ultrafiltration set
- Phenyl-SepharoseFF
- Amicon filters with UM-50 membrane
- Sodium phosphate buffer
- Sodium chloride
- ALPHA 1-4 LD (freeze dried)
- Trichloroacetic acid
- Nessler's reagent
- A549 cells (ATCC)

- RPMI 1640 medium (PanEco, Russia)
- Fetal bovine serum (PanEco, Russia)
- HEPES (PanEco, Russia)
- Sodium bicarbonate (PanEco, Russia)
- L-glutamine (PanEco, Russia)
- Streptomycin (PanEco, Russia)
- Penicillin (PanEco, Russia)
- Cisplatin (CDDP) (Ebewe Pharma Ges.m.b.H.Nfg.KG, Austria)
- Doxorubicin (DOX) (Veropharm, Russia)
- Flasks (Nunc)
- Plates (Nunc)
- 3-(4,5-dimethylthiazol-2-yl)-2,5-diphenyltetrazolium bromide (MTT) (Sigma-Aldrich)
- Pyridoxal-5-phosphate (PLP) (Sigma-Aldrich)
- Phosphate-buffered saline (PBS) (PanEco, Russia)
- Trypan blue (PanEco, Russia)
- Dimethylsulfoxide (DMSO) (PanEco, Russia)
- Athymic mice (Balb/c nude, female; 18–20 g; 6–8 weeks old) (N.N. Blokhin Cancer Research Center)
- SPSS 21 software

METHODS

Bacterial strains and culture conditions

1. Use *Escherichia coli* strain BL21 (DE3) F- *ompT hsdS* B *gal dcm* (DE3) (Novagen) to express the *C. sporogenes* MGL gene.
2. Grow bacteria in L-broth and on the agar medium at 37ºC.
3. Culture the transformed strains on media supplemented with kanamycin at a final concentration of 40 μg/ml.
4. Measure the optical density (OD) of the bacterial suspension at 590 nm using a KFK-2MP photocolorimeter.

5. Obtain the *E. coli* MDG1216 strain by the transformation of *E. coli* BL21 (DE3) cells with plasmid pET-mgl-Sporog [16].
6. After transformation, test *E. coli* MDG1216 clones for the ability to biosynthesize MGL and store in 40% glycerol in aliquots of 30 μl at –70 °C.
7. Use the working cell bank for growth of *E. coli* MDG1216.

MGL biosynthesis

8. Prepare inoculation medium containing tryptone (11.3 g/l), yeast extract (5.6 g/l) and glycerol (5.3 g/l). Grow *E. coli* MDG1216 strain in flasks (150 ml) at 37 ºC and 200 rpm up to OD=0.5 in this medium.
9. Carry out the biosynthesis of MGL by growing the *E. coli* MDG1216 strain in an ANCUM-2M fermenter (working volume 10 liters; Institute of Biological Instrumentation of RAS, Pushchino) for a total fermentation time of 12.5 h.
10. Obtain 0.45–0.52 kg of wet biomass with an MGL content of up to 45% of the total protein.

Purification

11. Thaw harvested *E. coli* MDG1216 cells (200 g) (stored at –70°C) and suspended in a 10 mM potassium-phosphate buffer with 0.001 M Na_4EDTA, 0.01% DTT and 0.01 мM pyridoxal phosphate, pH 7.2 (buffer 1) in the ratio of 1:5.
12. Disrupt the cells using an APV-1000 disintegrator with the addition of a PMSF solution in dioxane up to the final concentration of 1 mM.
13. Centrifuge the cell lysate and subject the supernatant to a heat treatment in 20% (vol.) ethanol.
14. Precipitate the admixtures by PEG 6000.
15. Load the obtained supernatant on a Q-Sepharose column (300 ml) equilibrated with buffer 1.
16. Elute the main peak from the column by 0.3 M KCl in the same buffer.
17. Ultrafilter (VivaFlow set) the collected peak fractions using a membrane module with the cut-off threshold of 50 kDa.
18. Increase the KCl content in the retentate up to 1 M and add the obtained solution to a column of Phenyl-SepharoseFF (25 ml) equilibrated with buffer 1 containing 1 M KCl such that the MGL does not bind to the sorbent under the above conditions and flows through the column.

19. Concentrate the MGL-containing fraction with Amicon using the UM-50 membrane.
20. Enhance the content of KCl in the retentate up to 1.5 M and load the solution on a column of Phenyl-Sepharose FF (50 ml) equilibrated with buffer 1 containing 1.5 M KCl.
21. Elute the MGL from the column by decreasing the salt concentration up to 0.75 M in the buffer.
22. Desalinate the MGL solution and transfer to a 20 mM sodium phosphate buffer containing 0.15 M sodium chloride and 0.01 mM pyridoxal phosphate, pH 7.2, by ultra-diafiltration on the VivaFlow set using a membrane with a 50 kDa cut-off.
23. Add Tregalose to the obtained protein solution in the ratio 1.5:1 (vol./vol.).
24. Subject the final product to sterilizing filtration.
25. Bottle the sterile solution in dark-glass vials (2000±200 MU per vial) and freeze-dry (ALPHA 1-4 LD).
26. Cap the ready-made vials for labeling and storage at 2–8°C.
27. Use SDS-PAGE for homogeneity and purity determination of the MGL (Figure 1).

Figure 1.

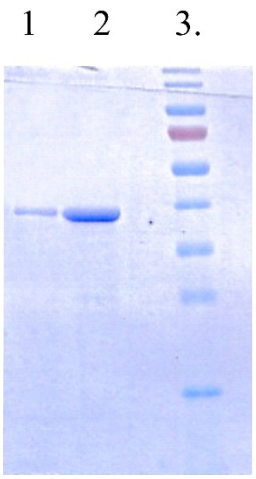

Figure 1. SDS-PAGE for homogeneity and purity determination of MGL. (1) 0.2 µg MGL; (2) 4 µg MGL; (3) Protein markers (Fermentas, #SM0671).

Enzymatic assay

28. Constitute a reaction mixture of the 304 µl of working buffer (100 mM potassium phosphate buffer (pH 8.0), containing 0.01 mM pyridoxal phosphate and 0.01% dithiothreitol) and 76 µl 100 mM L-methionine.

29. Initiate the reaction by the addition of 20 µl of purified enzyme (2 mg/ml).
30. Incubate the reaction mixture at 37 °C for 1 min and stop the reaction by adding 100 µl of 1.5 M trichloroacetic acid.
31. Centrifuge the reaction mixture at 10000 g for 5 min at 4 °C to remove the precipitates.
32. Determine the ammonia released in supernatant using a colorimetric technique by adding 50 µl Nessler's reagent into the sample containing 50 µl supernatant and 1150 µl distilled water.
33. Vortex the contents in the sample and incubate at room temperature for 12 min and measure the OD at 450 nm.
34. Determine the ammonia produced in the reaction based on the standard curve obtained with ammonium sulfate.
35. Define one unit (U) of MGL activity as the amount of the enzyme that liberates one µmol of ammonia per min at 37 °C.
36. By this isolation and purification procedure, obtain an enzyme with a specific activity of 25.8–27.7 U/mg.

Cell lines and cell viability assay

37. Grow A549 human lung cancer cells in RPMI 1640 medium with supplements in flasks at 37 °C and 5% CO_2.
38. After 80% confluency, trypsinize the cells in exponential growth phase and suspend in fresh medium supplemented with 5×10^{-5} M pyridoxal-L-phosphate (PLP) and seed to the 96-well plates in concentration 4×10^{5} cell/ml.
39. Count the cells after treating with 0.4% trypan blue solution.
40. After 24 h, add different concentration of tested drugs dissolved in PBS in wells.
41. Expose cells to different concentrations of CDDP, DOX, MGL, alone and in combination, for 72 h.
42. Add PBS only in control wells with untreated cells.
43. Estimate the cell viability by MTT assay as described in [17].
44. Measure the absorbance of DMSO with dissolved MTT–formazan crystals at 540 nm (Multiscan, Finland).
45. Express the results as of the drug concentration that inhibited 50% cell growth.

46. Calculate the EC_{50} values from the concentration-effect relationships using Combenefit software.

Animal experiments

47. Conduct all animal experiments in accordance with the internationally accepted principles for laboratory animal use and care, as described in the European Economic Community (EEC) guidelines (EEC Directive of 1986; 86/609/EEC), and with approval from the Ethics Committee for Animal Experimentation of N.N. Blokhin Cancer Research Center.
48. Subcutaneously inject A549, MCF7 or SKBR3 cells (2×10^6 cells) into the flank of the mice for tumor formation.
49. Detect established tumors of ~100 mm^3 ±10% in volume.
50. Randomly assign the mice to treatment arms and treated as follows: i) 0.2 ml saline alone i.p. daily; ii) MGL at 1000 U/kg daily × 10 i.p., as determined by preliminary experiments (data not published); iii) DOX 2 mg/kg every other day × 5 i.p.; iv); CDDP 1.5 mg/kg every other day × 5 i.p.; v) combination of (ii and iii); and vi) combination of (ii and iv).
51. Assess tumor volume three times a week using a calipers, measuring three perpendicular diameters, and measure the body weights every 4 days.
52. Calculate the tumor inhibitory ratio using the following formula: TGI (tumor growth inhibition, %)=[(C–T)/C]×100, where C is the mean tumor size of the solvent control group and T is the mean tumor size of the treated group.

Analysis of combined drug effects

53. Analyze the drug combination effect by the method of Chou and Talalay [15] with calculation of combination index (CI). The CI indicates antagonism (CI>1), additivity (CI=1), or synergism (CI<1).
54. Calculate the modified coefficient of drug interaction (CDI) according to [18] where CDI<1, = 1 or >1 indicates that the drugs are synergistic, additive or antagonistic, respectively. CDI <0.7 indicates that the drug is significantly synergistic.
55. Use average-CDI to evaluate the total drug combination effect [19].

Statistical analysis

56. Repeat experiments *in vitro* until three replicates yielded coefficients $R > 0.9$ for all three median effect lines.
57. Make calculations of CI and average-CDI values with Microsoft Office Excel 2010, EC50 values — with Combenefit software.
58. Use the Loewe and Bliss models for synergy/antagonism drug combination effect analysis.
59. Use SPSS 21 software for statistical analysis for in vivo experiments.
60. Use one-way ANOVA to compare efficacy of monotherapy and combined therapy.
61. Perform post hoc Dunnett`s test to assess differences between the individual groups against one control.
62. Use the Dunnett`s T3 test to assess differences between the individual groups. P value <0.05 was considered statistically significant.

RESULTS

EC_{50} of MGL against A549, SK-BR3, SCOV3 and MCF7 human cancer cell lines

The calculated EC_{50} values for MGL were 4.4 U/ml for A549; 7.5 U/ml for SK-BR3; 2.4 U/ml for SKOV3; 0.4 U/ml for MCF7.

MGL synergistically enhances the cytotoxicity of CDDP on A549 cells

Three different mixtures, namely CDDP+MGL (5 U), CDDP+MGL (2.5 U), and CDDP+MGL (1.25 U), were used to analyze the mutual inhibitory effect of drug combination when compared with MGL and CDDP alone (**Figure 2**). The concentration of CDDP ranged from 0 to 50 μg/ml, whereas the activity of the enzyme was constant (5 U or 2.5 U or 1.25 U).

Figure 2.

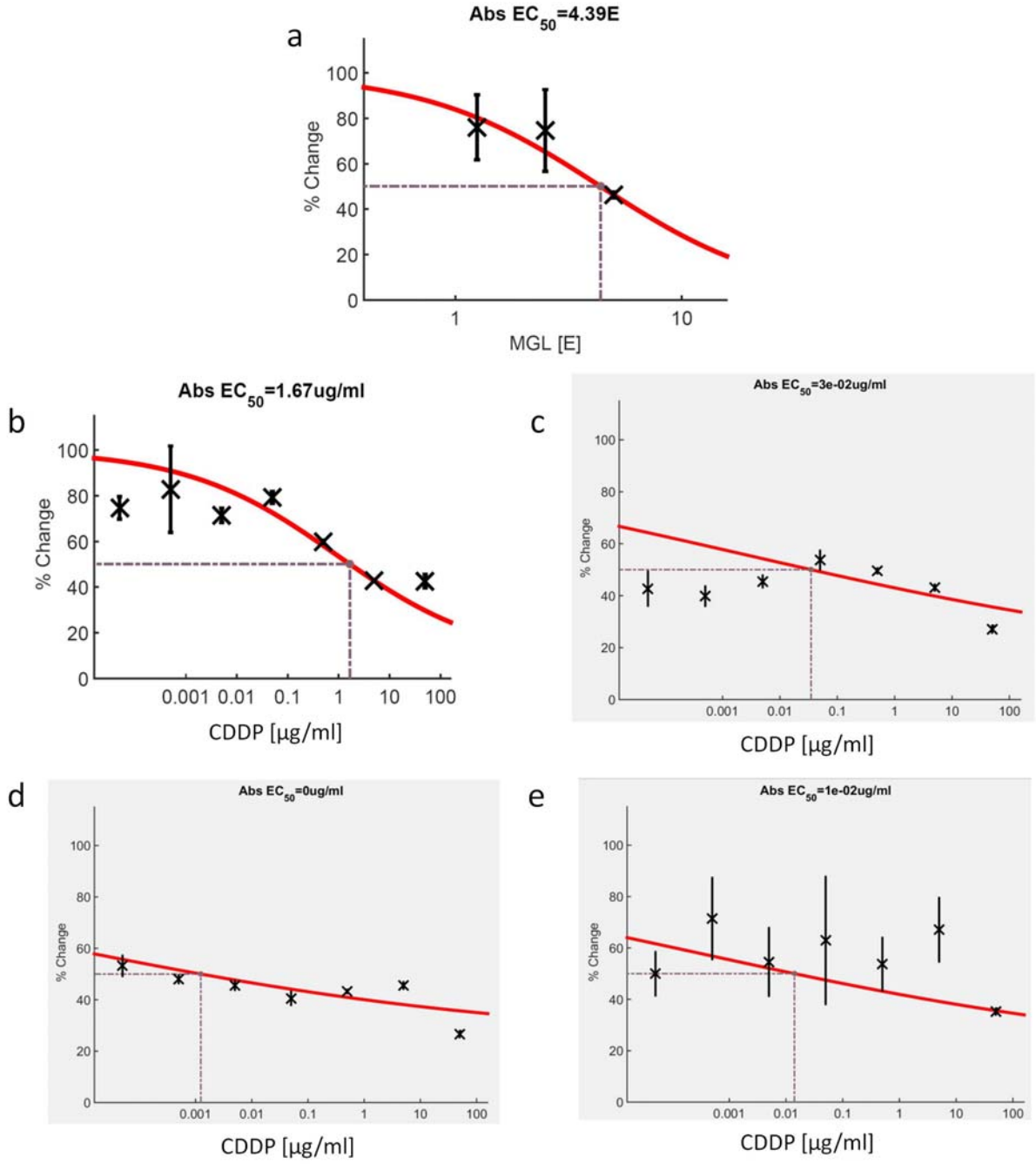

Figure 2. EC_{50} values of MGL and CDDP, and CDDP+MGL combinations on A54 cells calculated by Combenefit software: a) MGL; b) CDDP alone; c) CDDP+MGL 1.25 U; d) CDDP+MGL 2.5 U; e) CDDP+MGL 5 U.

As shown on **Figure 3** and **Table 2** CDDP+MGL 5 U and CDDP+MGL 2.5 U combinations demonstrated higher cytotoxicity on A549 cells compared with CDDP alone in low concentrations (0–0.5 μg/ml).

Figure 3.

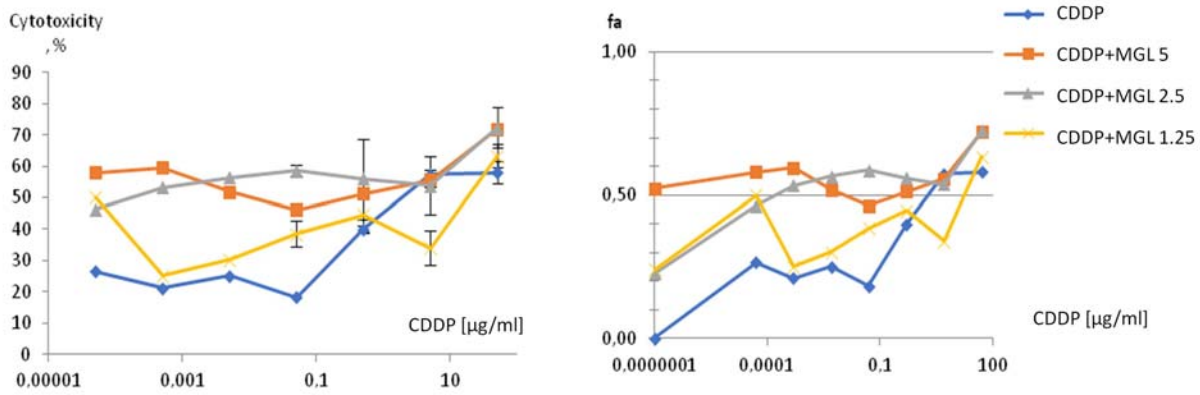

Figure 3. Cytotoxic activity of CDDP+MGL combinations versus CDDP alone on A549 cells. a) cytotoxicity, %; b) fa — a desired fractional affected cell kill.

Table 2. Combination effect of CDDP and MGL

Tested drugs	EC_{50}	CI		Average-CDI	
MGL	4.39 U	–	–	–	–
CDDP	1.67 μg/ml	–	–	–	–
CDDP+MGL 5 U	0.03 μg/ml	1.18	Additive or antagonistic	0.95	Additive
CDDP+MGL 2.5 U	0.002 μg/ml	0.68	Synergistic	0.74	Synergistic
CDDP+MGL 1.25 U	0.01 μg/ml	0.69	Synergistic	0.78	Synergistic

CI and average CDI values are shown in **Table 1**. The efficacy of CDDP+MGL 2.5 U and CDDP+MGL 1.25 U on A549 cells are synergistic (average CDI –0.74 and 0.78, respectively); CDDP+MGL 5 U are additive (average CDI –0.95). CDDP+MGL 2.5 U are more synergistic

with a lower concentration of CDDP: EC_{50} of CDDP in CDDP+MGL 2.5 U = 0.002 µg/ml vs 0.01 µg/ml (CDDP+MGL 1.25 U), 0.03 µg/ml (CDDP+MGL 5 U), 1.67 µg/ml (CDDP), 4.39 µg/ml (MGL). Key results of this analysis are presented in **Figure 4**.

Figure 4.

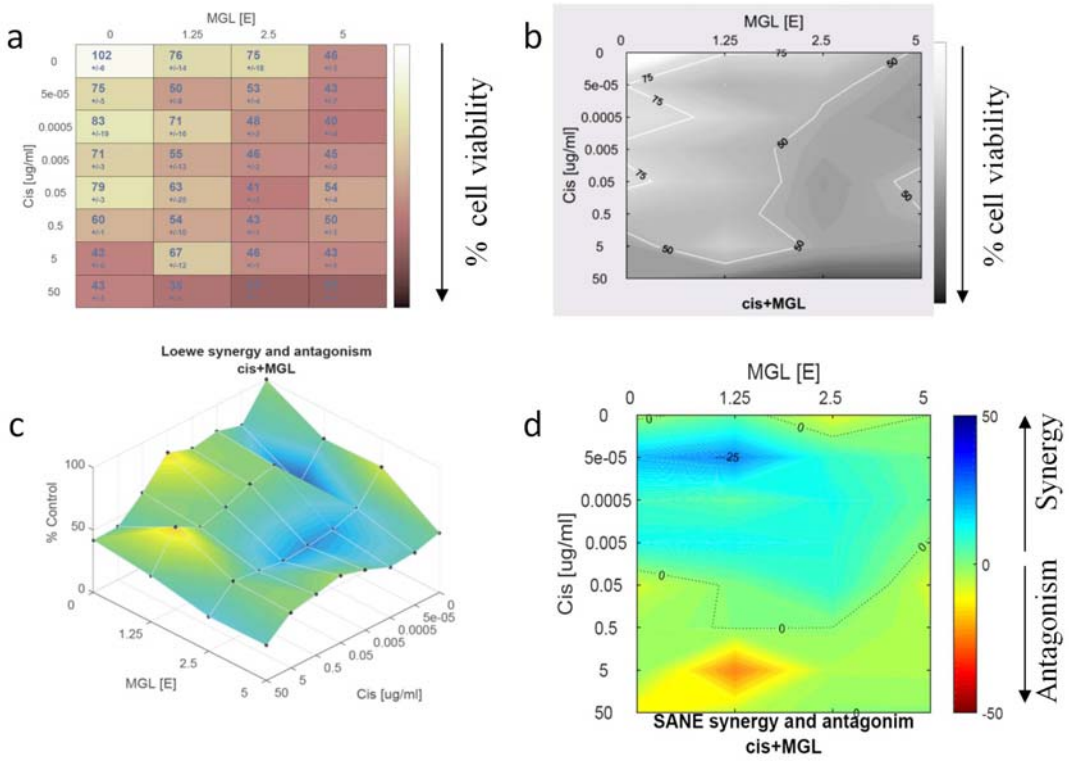

Figure 4. Analysis of CDDP and MGL combination effect on % A549 cell viability: a) Detailed analysis of cell survival after incubation with different concentrations of drugs; b) Contour Sane synergy and antagonism model of influence of CDDP and MGL to % cell viability; c) Loewe mapped surface model for analysis of the influence concentration of components to effect of mixtures; d) contour Loewe synergy and antagonism model of influence of CDDP and MGL to % cell viability.

MGL synergistically enhances the cytotoxicity of DOX in A549 cells

To investigate the effects of MGL and DOX on the proliferation of A549 cells, three different mixtures, namely DOX+MGL (5 U), DOX+MGL (2.5 U), and DOX+MGL (1.25 U), were used (**Figure 5**). In each mixture the concentration of DOX ranged from 0 to 100 µg/ml, whereas the activity of the enzyme was constant (5 U or 2.5 U or 1.25 U).

Figure 5.

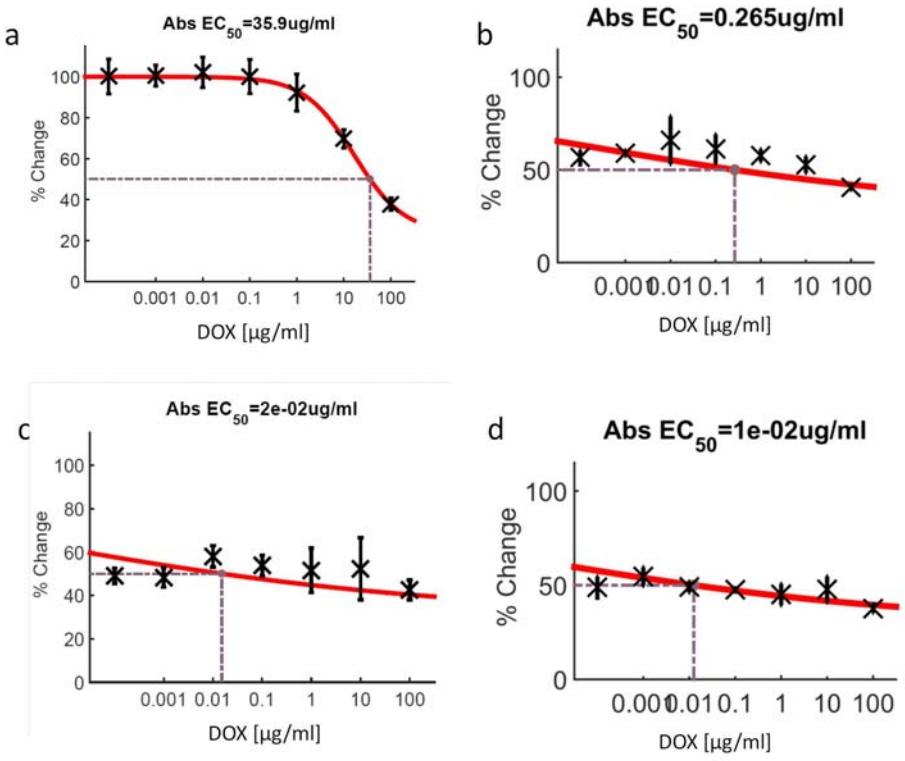

Figure 5. EC_{50} values of DOX and DOX+MGL mixtures on A549 cells calculated using Combenefit software: a) DOX alone; b) DOX + MGL 1.25 U; c) DOX + MGL 2.5 U; d) DOX + MGL 5 U.

As shown on **Figure 6 and 7** and **Table 3** all combinations of DOX+MGL demonstrated higher cytotoxicity when compared with DOX alone in 0–10 µg/ml concentrations.

Figure 6.

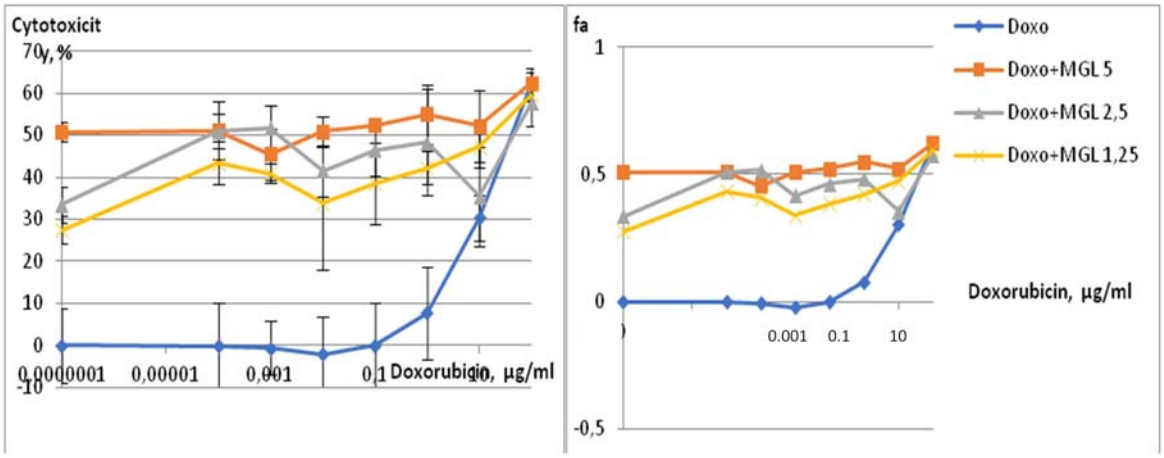

Figure 6. Cytotoxic activity of DOX+MGL combinations versus DOX alone on A549 cells. a) cytotoxicity, %; b) fa — desired fractional affected cell kill.

Table 3. Combination effect of DOX and MGL on A549 cells

Tested drugs	EC_{50}	CI		Average-CDI	
DOX	35.9 µg/ml	–	–	–	–
DOX+MGL 5 U	0.01 µg/ml	1.011	Additive	0.97	Additive
DOX+MGL 2.5 U	0.02 µg/ml	1.002	Additive	0.89	Additive or synergistic
DOX+MGL 1.25 U	0.265 µg/ml	0.740	Synergistic	0.85	Synergistic

Effect of DOX+MGL 1.25 U can be interpreted as synergistic when compared with DOX alone: CI corresponded to 0.74, average-CDI –0.85. Effect of DOX + MGL 2.5 U and DOX + MGL 5 U was defined as additive.

Figure 7.

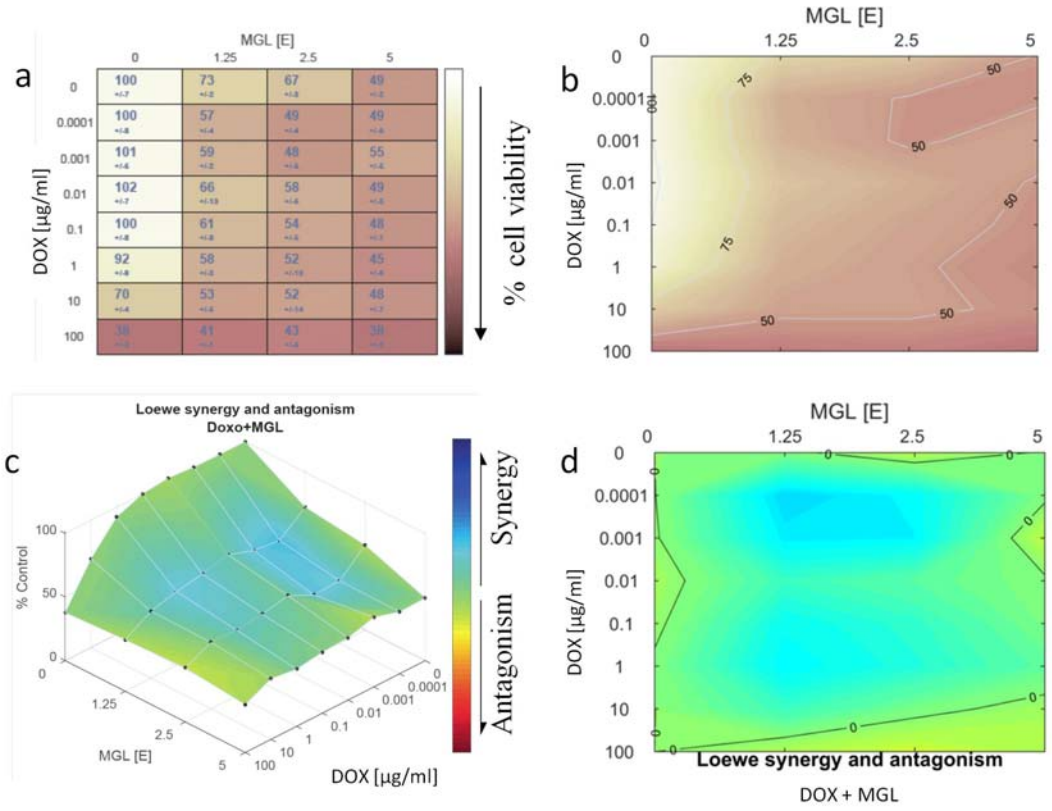

Figure 7. Cell viability after co-incubation with MGL and DOX on A549 cells: a and b) Analysis of cell survival with different concentrations of drugs; c) contour Loewe synergy and antagonism model of influence of DOX and MGL on cell viability, %; d) Loewe mapped surface model for analysis of the influence concentration of components to effect of mixtures.

MGL induces additive cytotoxic effect in SK-BR3 and SCOV-3 cell lines when combined with CDDP and DOX

CDDP or DOX + MGL combinations were studied in SK-BR-3 and SCOV-3 cell lines. It was found that the DOX + MGL 5 or 2.5 U and CDDP + MGL 5 or 2.5 U combinations had a low synergistic effect against SK-BR3: average-CDI values of DOX + MGL 5 U = 0.81; DOX + MGL 2.5 U =0.79; CDDP + MGL 5 U = 0.71; CDDP + MGL 2.5 U = 0.84. For SK-BR3, CDDP + MGL 1.25 U and DOX + MGL 1.25 U showed an additive effect: average-CDI values were 1.02 and 1.16, respectively (**Table 4**).

The effect of the combined treatment of tested cytotoxic agents with 1.25 U MGL and 5 U MGL on SCOV-3 was defined as antagonistic: average-CDI values varied from 1.11 to 1.32. Effect of DOX + MGL 2.5 U and CDDP + MGL 2.5 U tested on SCOV-3 cells was additive: average-CDI values were equal to 1.08 and 1.09 (**Table 5**).

Table 4. Cytotoxicity of DOX or CDDP + MGL against SK-BR-3

Substance	DOX + MGL		CDDP + MGL	
	EC_{50}	Average-CDI	EC_{50}	Average-CDI
MGL alone	2.4 U	-	-	-
Drug alone	2 µg/ml	-	0.59	-
Drug + MGL 5 U	0.06 µg/ml	0.81	0.41	0.71
Drug + MGL 2.5 U	0.07 µg/ml	0.79	1.87	0.84
Drug + MGL 1.25 U	0.29 µg/ml	1.02	2.53	1.16

Table 5. Cytotoxicity of DOX or CDDP + MGL against SCOV-3

Substance	DOX + MGL		CDDP + MGL	
	EC_{50}	Average-CDI	EC_{50}	Average-CDI
MGL alone	4.4 U	-	-	-
Drug alone	0.07 µg/ml	-	1.5	-
Drug + MGL 5 U	0.07 µg/ml	1.27	1.7	1.32
Drug + MGL 2.5 U	0.31 µg/ml	1.08	0.6	1.09
Drug + MGL 1.25 U	1.0 µg/ml	1.11	0.5	1.28

MGL does not increase the cytotoxicity of other cytotoxic agents in vitro

We investigated the possible effect of MGL on cytotoxicity of carboplatin, vincristine, cyclophosphamide, gemcitabine, etoposide, docetaxel, dacarbazine, and irinotecan. We were unable to detect a significant change of cytotoxicity of these agents when combined with MGL.

MGL inhibits growth of SK-BR3 xenografts similar to DOX and CDDP

Mice were transplanted with SK-BR-3 cells to establish the subcutaneous xenografts. The initial tumor volume in each group was ~110 mm^3 ±10% (range from 98.3 to 120.9 mm^3, day 1, treatment onset). At the end of the treatment (day 10), the average volume of the tumor reached 1172.3±742.1 mm^3 in the control (vehicle) arm; 584.5±215.1 mm^3 in the MGL arm (TGI 50%); 401.3±179.7 mm^3 in the DOX arm (TGI 66%); 560.6±162.1 in the CDDP arm (TGI 52%); and 561.7±247.0 mm^3 and 529.3±144.9 in the combined DOX + MGL and CDDP + MGL arms (TGI 52 and 55%, respectively). No statistically-significant differences were observed between treatment arms (**Figure 8**) (**Note 2**).

Figure 8.

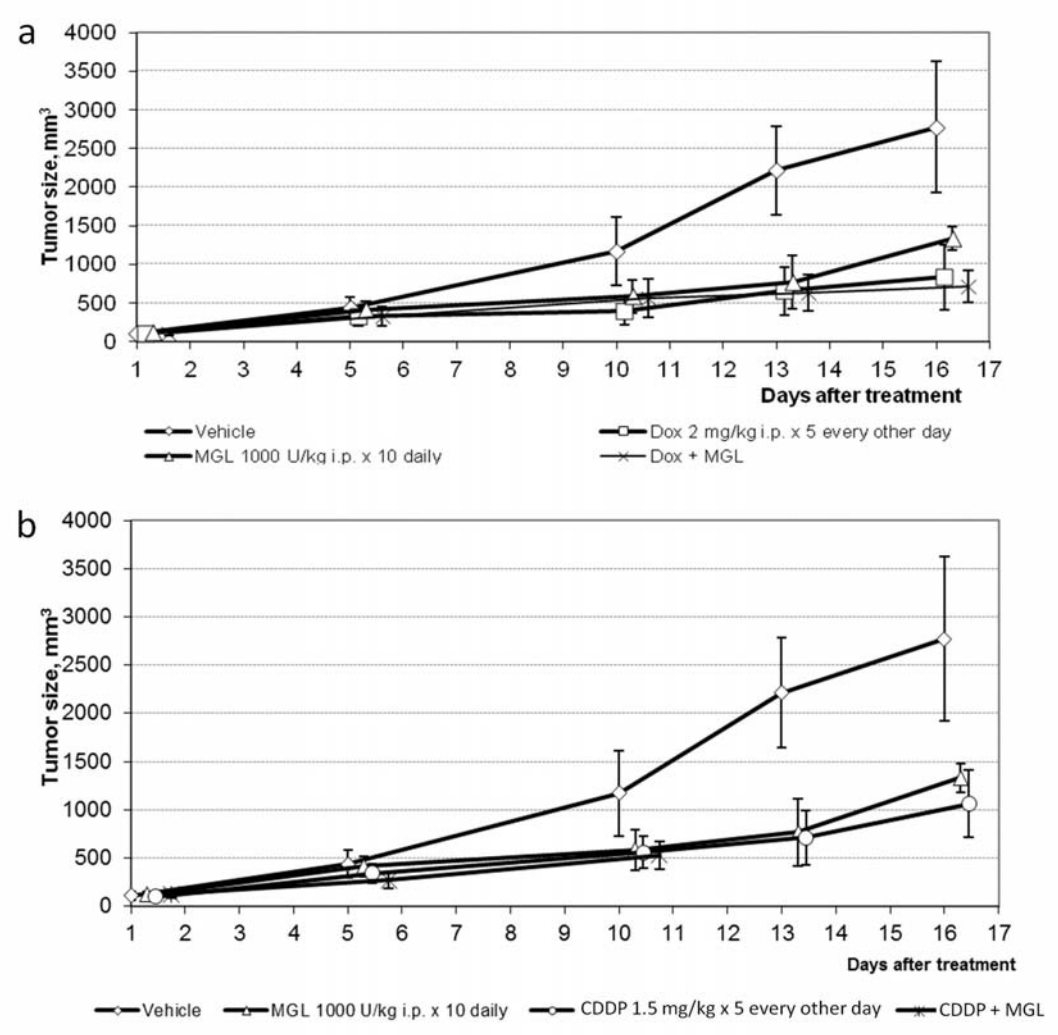

Figure 8. Efficacy of MGL alone or with DOX (a) or CDDP (b) on SK-BR3 xenografts. Breast cancer xenograft. SK-BR3 cells (7×10^6 cells) were injected subcutaneously into both flanks of nude mouse (5 mice/group). After tumors were established, mice were treated with 2 mg/kg DOX or 1.5 mg/kg CDDP *i.p.* every other day × 5, and 1000 U/kg MGL *i.p.* daily × 10 as single agents or in combination.

MGL inhibits growth of MCF7 xenografts similar to CDDP or DOX

On day 1 (onset of treatment) initial xenograft volume reached ~100 mm^3, and mice were randomly assigned to 6 arms. At the end of treatment (day 10), the volume of the tumor mass was 506.6±269.4 mm^3 in the control (vehicle) arm; 134.5±75.4 mm^3 in the MGL arm (TGI 74%, p=0.037); 114.5±55.3 mm^3 in DOX arm (TGI 77%, p=0.029); 162.6±84.4 in CDDP arm (TGI

68%, p=0,046); and 125.7±80.4 mm^3 and 219.4±68.0 mm^3in the combined DOX + MGL or CDDP + MGL arms (TGI 75%, p=0.033 and 57%, p=0.118, respectively). No statistically significant differences between treatment arms were observed (**Figure 9**).

Figure 9.

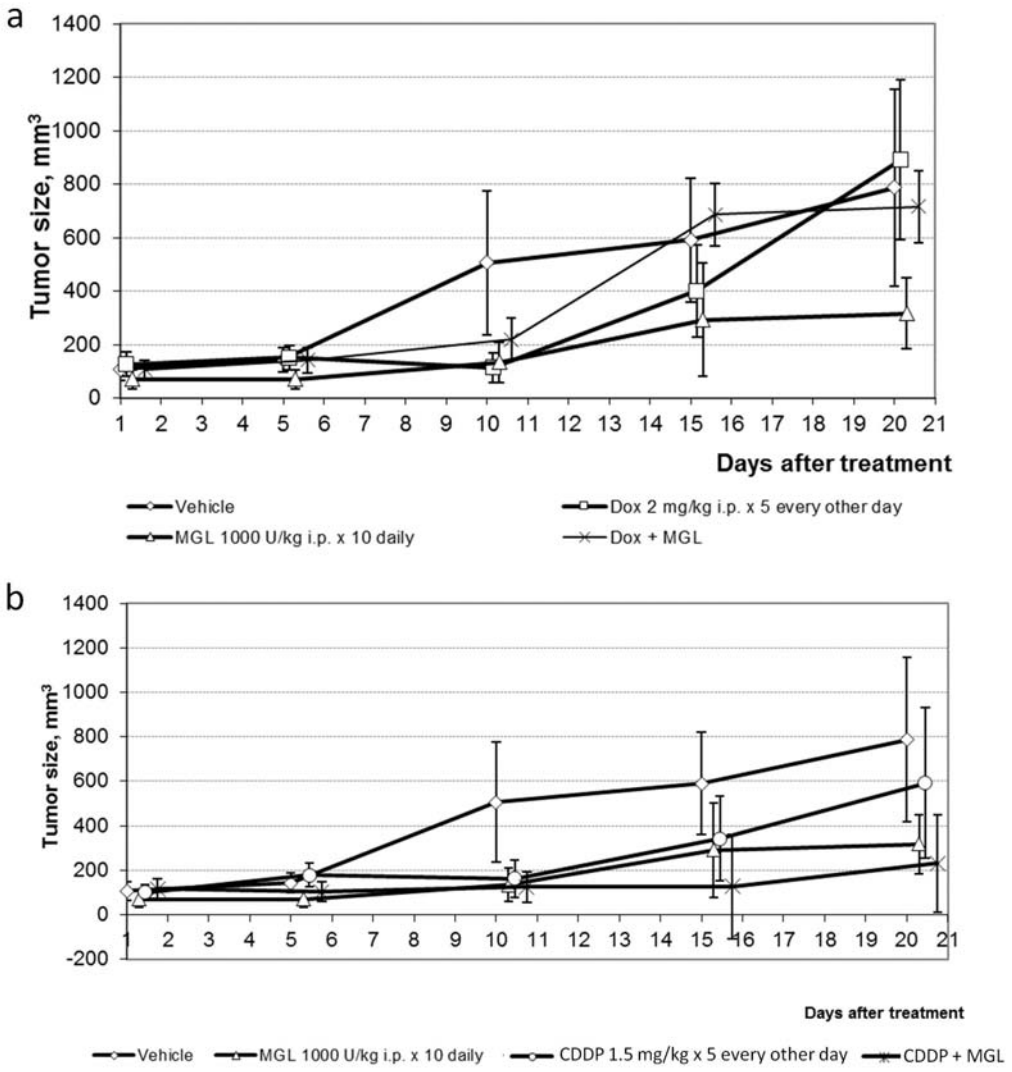

Figure 9. Efficacy of MGL alone or with DOX (a) or CDDP (b) on MCF7 xenografts. Breast cancer xenograft MCF7 cells (7□×□10^6 cells) were injected subcutaneously into both flanks of nude mouse (5 mice/group). After tumors were established, mice were treated with 2 mg/kg DOX or 1.5 mg/kg CDDP *i.p.* every other day × 5, and 1000 U/kg MGL *i.p.* daily × 10 as single agents or in combination.

MGL in combination with DOX significantly decreases the tumor growth in A549 xenografts

On day 1 (onset of treatment) initial xenograft volume was ~150 mm^3, and mice were randomly assigned to 4 arms. Four days after the end of treatment (day 14), the volume of the tumor mass reached 1996.0±200.0 mm^3 in the control (vehicle) arm; 1221.6±177.3 mm^3 in the MGL arm (TGI 39%, p=0,045, Dunnet T3); 1598.7±202.5 mm^3 in the DOX arm (TGI 20%, p=0,660); and 858.9±123.0 mm^3 in the combined DOX + MGL arm (TGI 57%, p<0,001). Co-treatment with MGL and DOX significantly decreased the tumor volume compared to single treatment with MGL or DOX in A549 tumors. The inhibition rates of tumor growth in the combined arm was 57%, which was significantly greater than those in the DOX arm (p=0.033), but not MGL alone arm (p=0.657). None of the mice exhibited signs of physical discomfort during the treatment and follow-up periods. These results suggest that combination of MGL and DOX may significantly inhibit tumor growth *in vivo* (**Notes 2, 3**).

Figure 10.

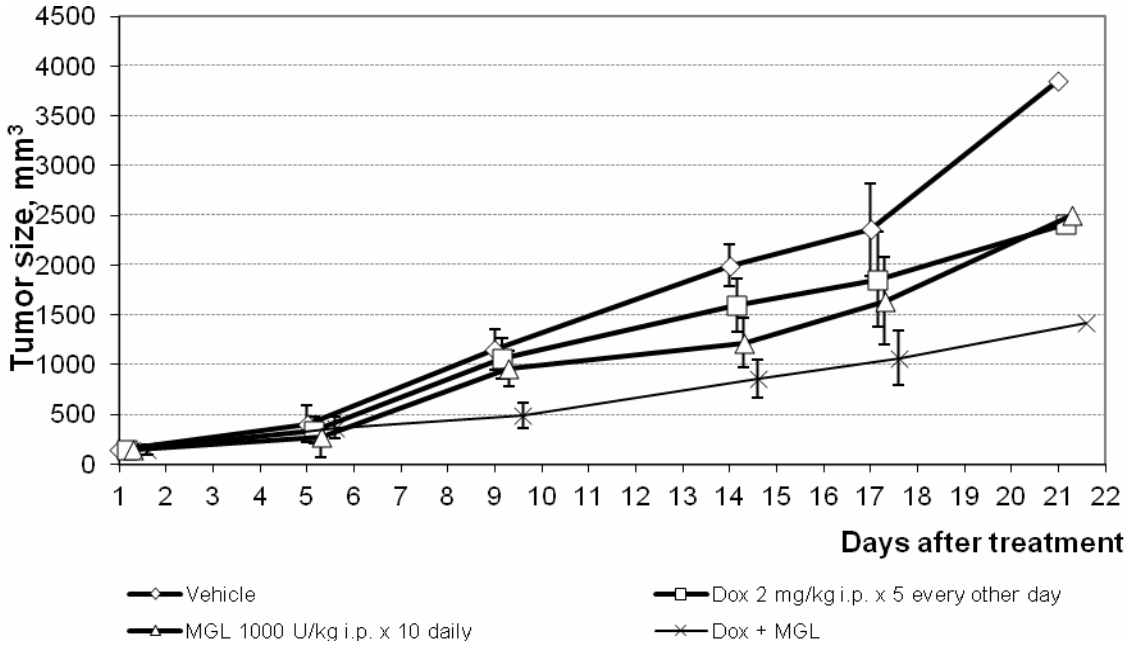

Figure 10. Efficacy of DOX + MGL combination in A549 xenograft model. NSCLC xenograft. A549 cells (7×10^6 cells) were injected subcutaneously into both flanks of nude mouse

(5 mice/group). After tumors were established, mice were treated with 2 mg/kg DOX *i.p.* every other day × 5, and 1000 U/kg MGL *i.p*. daily × 10 as single agents or in combination.

Notes

Note 1: A number of amino acid cleaving enzymes has been studied in recent years, reflecting amino acid dependence as a general metabolic defect in caner, which preclude the cells from growing in media in which certain amino acid is depleted. These enzymes include novel asparaginases [19-21], lysine alpha-oxidase [22], phenylalanine ammonia-lyase [23] and MGL. Methionine dependence, the essential methionine requirement for cell growth, occurs frequently in many types of human cancer cell lines and animal models of cancer [24-28].

Note 2: Reduction of plasma methionine below 5 mM arrests human xenograft growth in athymic mice [13], suggesting that that plasma methionine level of <5 mM may be necessary to achieve significant anticancer effect in an animal model. We reported previously $T_{1/2}$ of MGL from *C. sporogenes* after intravenous injection into mice is 1.31±0.03 h. Mouse plasma methionine decreased to an undetectable level 10 min after 1000 U/kg injection. This effect persisted for 6 hours, indicating the feasibility of long-term reduction of methionine to a negligible level (<5 μM) [29].

Note 3: In our study, we found that combination of DOX and MGL is more effective in A549 tumor growth inhibition than either agent alone. The growth inhibitory effect of DOX + MGL on A549 xenograft *in vivo* was reflective of the results obtained *in vitro*, whereas the statistically significant regression of xenografts was not achieved using a single treatment with either MGL or DOX. Future studies are required to further investigate cellular mechanisms of potential of cytotoxic agents to increase MGL efficacy and to optimize the treatment schedule to achieve complete tumor regression.

References

1. El-Sayed A.S. Microbial L-methioninase: production, molecular characterization, and therapeutic applications. Appl Microbiol Biotechnol. 2010;86:445-467.
2. Cellarier E., Durando X., Vasson M.P., et al. Methionine dependency and cancer treatment. Cancer Treat Rev. 2003;29:488–489.
3. Hoffman R.M. Development of recombinant methioninase to target the general cancer-specific metabolic defect of methionine dependence: a 40-year odyssey, Expert Opin. Biol. Ther. 2015;15:21–31.
4. Kreis W., Hession C. Biological effects of enzymatic deprivation of L-methionine in cell culture and an experimental tumor. Cancer Res. 1973;33:1866-1869.
5. Yoshioka T., Wada T., Uchida N., et al. Anticancer efficacy in vivo and in vitro, synergy with 5-fluorouracil and safety of recombinant methioninase. Cancer Res 1998;58:2583–7.
6. Tan Y., Sun X., Xu M., et al. Efficacy of recombinant methioninase in combination with cisplatin on human colon tumors in nude mice. Clin Cancer Res 1999;5:2157–63.
7. Kokkinakis D.M., Wick J.B., Zhou Q.-X. Metabolic response of normal and malignant tissue to acute and chronic methionine stress in athymic mice bearing human glial tumor xenografts. Chem Res Toxicol 2002;15:1472–9.
8. Murakami T., Li S., Han Q., et al. Recombinant methioninase effectively targets a Ewing's sarcoma in a patient-derived orthotopic xenograft (PDOX) nude-mouse model. Oncotarget 2017;8:35630-35638.
9. Kawaguchi K., Igarashi K., Li S., et al. Combination treatment with recombinant methioninase enables temozolomide to arrest a BRAF V600E melanoma growth in a patient-derived orthotopic xenograft. Oncotarget 2017;8:85516-85525.
10. Igarashi K., Kawaguchi K., Li S., et al. Recombinant methioninase in combination with DOX overcomes first-line DOX resistance in a patient-derived orthotopic xenograft nude-mouse model of undifferentiated spindle-cell sarcoma. Cancer Letters 2018;417:168-173.
11. El-Sayed A.S., Shouman S.A., Nassrat H.M. Pharmacokinetics, immunogenicity and anticancer efficiency of Aspergillus flavipes L-methioninase. Enzyme Microb Technol. 2012; 51(4):200-10.

12. Stern P.H., Hoffman R.M. Enhanced in vitro selective toxicity of chemotherapeutic agents for human cancer cells based on a metabolic defect. J Natl Cancer Inst (Bethesda) 1986;76:629–39.
13. Kokkinakis D.M., Schold S.C.J., Hori H., Nobori T. Effect of long-term depletion of plasma methionine on the growth and survival of human brain tumor xenografts in athymic mice. Nutr Cancer 1997;29:195–204.
14. Kokkinakis D.M., Hoffman R.M., Frenkel E.P., et al. Synergy between methionine stress and chemotherapy in the treatment of brain tumor xenografts in athymic mice. Cancer Res 2001;61:4017–23.
15. Morozova E.A., Kulikova V.V., Yashin D.V. et al. Kinetic Parameters and Cytotoxic Activity of Recombinant Methionine γ-Lyase from Clostridium tetani, Clostridium sporogenes, Porphyromonas gingivalis and Citrobacter freundii. Acta Naturae. 2013;5(3):92-8.
16. Anufrieva N.V., Morozova E.A., Kulikova V.V. et al. Sulfoxides, Analogues of L-Methionine and L-Cysteine As Pro-Drugs against Gram-Positive and Gram-Negative Bacteria. Acta Naturae. 2015;7(4):128-35.
17. Pokrovskaya M.V., Pokrovskiy V.S., Aleksandrova S.S., et al. Recombinant intracellular Rhodospirillum rubrum L-asparaginase with low L-glutaminase activity and antiproliferative effect. Biochemistry (Moscow) Supplement. Series B: Biomedical Chemistry 2012;6(2):123-131.
18. Wang W.T., Zhao Y., Gao J.L. et al. Cytotoxicity enhancement in MDA-MB-231 cells by the combination treatment of tetrahydropalmatine and berberine derived from Corydalis yanhusuo Intercult Ethnopharmacol. 2014;3(2):68-72.
19. Sidoruk K.V., Pokrovsky V.S., Borisova A.A. et al. Creation of a producent, optimization of expression, and purification of recombinant Yersinia pseudotuberculosis L-asparaginase. Bull Exp Biol Med. 2011;152(2):219-23
20. Pokrovskaya M.V., Aleksandrova S.S., Pokrovsky V.S. et al. Identification of functional regions in the Rhodospirillum rubrum L-asparaginase by site-directed mutagenesis. Mol Biotechnol. 2015;57(3):251-64.

21. Pokrovsky V.S., Kazanov M.D., Dyakov I.N. et al. Comparative immunogenicity and structural analysis of epitopes of different bacterial L-asparaginases. BMC Cancer. 2016;16:89.
22. Sannikova E.P., Bulushova N.V., Cheperegin S.E. et al. The Modified Heparin-Binding L-Asparaginase of Wolinella succinogenes. Mol Biotechnol. 2016;58(8-9):528-39.
23. Pokrovsky V.S., Treshalina H.M., Lukasheva E.V. et al. Enzymatic properties and anticancer activity of L-lysine α-oxidase from Trichoderma cf. aureoviride Rifai BKMF-4268D.Anticancer Drugs. 2013;24(8):846-51.
24. Babich O.O., Pokrovsky V.S., Anisimova N.Y. et al. Recombinant l-phenylalanine ammonia lyase from Rhodosporidium toruloides as a potential anticancer agent. Biotechnol Appl Biochem. 2013;60(3):316-22.
25. Mecham J.O., Rowitch D., Wallace C.D. et al. The metabolic defect of methionine dependence occurs frequently in human tumor cell lines. Biochem Biophys Res Commun 1983;117:429–34.
26. Hoffman R.M., Erbe R.W. High in vivo rates of methionine biosynthesis in transformed human and malignant rat cells auxotrophic for methionine. Proc Natl Acad Sci USA 1976;73:1523–7.
27. Hoffman R.M. Altered methionine metabolism, DNA methylation, and oncogene expression in carcinogenesis: a review and symthesis. Biochim Biophys Acta 1984;738:49–87.
28. Guo H., Herrera H., Groce A., Hoffman R.M. Expression of the biochemical defect of methionine dependence in fresh patient tumors in primary histoculture. Cancer Res 1993;53:2479–83.
29. Tisdale M, Eridani S. Methionine requirement of normal and leukaemic haemopoietic cells in short term cultures. Leuk Res 1981;5: 385–94.